

# Tissue-engineered autologous peritoneal grafts for bladder reconstruction in a porcine model

Journal of Tissue Engineering  
Volume 12: 1–12  
© The Author(s) 2021  
Article reuse guidelines:  
sagepub.com/journals-permissions  
DOI: 10.1177/2041731420986796  
journals.sagepub.com/home/tej



Biao Chen<sup>1,2\*</sup>, Xia Chen<sup>3\*</sup>, Wenjia Wang<sup>2</sup>, Jun Shen<sup>4</sup>,  
Zhiqiang Song<sup>2</sup>, Haoyu Ji<sup>1,2</sup>, Fangyuan Zhang<sup>1,2</sup>,  
Jianchen Wu<sup>2</sup>, Jie Na<sup>3</sup>  and Shengwen Li<sup>1,2</sup>

## Abstract

Ileal neobladder construction is a common treatment for patients with bladder cancer after radical cystectomy. However, metabolic disorders caused by transposed bowel segments occur frequently. Bladder tissue engineering is a promising alternative approach. Although numerous studies have reported bladder reconstruction using acellular and cellular scaffolds, there are also disadvantages associated with these methods, such as immunogenicity of synthetic grafts and incompatible mechanical properties of the biomaterials. Here, we engineered an autologous peritoneal graft consisting of a peritoneal sheet and the seromuscular layer from the ileum. Three months after the surgery, compared with the neobladder made from the ileum, the reconstructed neobladder using our new method showed normal function and better gross morphological characteristics. Moreover, histopathological and transcriptomic analysis revealed urothelium-like cells expressing urothelial biomarkers appeared in the neobladder, while no such changes were observed in the control group. Overall, our study provides a new strategy for bladder tissue engineering and informs a variety of future research prospects.

## Keywords

Autologous tissue engineering, peritoneum, bladder reconstruction, urinary diversion, cell differentiation

Date received: 19 August 2020; accepted: 18 December 2020

## Introduction

Bladder cancer is the second most common urologic cancer worldwide.<sup>1</sup> Muscle-invasive bladder cancer accounts for 30% of cases in newly diagnosed patients.<sup>2</sup> Most of these patients are treated with radical cystectomy and intestinal urinary diversion. Orthotopic neobladder has been established as the most common type of urinary diversion in pioneering urologic oncology centers.<sup>3</sup>

Gastrointestinal segments remain the primary source of material for urinary tract reconstruction. However, the transposed intestine segments maintain their absorption and secretion functions after replacing the urinary tract, which will lead to adverse consequences.<sup>4</sup> Firstly, long-term exposure of the intestinal mucosa to urine may lead to metabolic acidosis, which has been noted in 70% of patients in the early postoperative period.<sup>5</sup> Secondly, there has been increasing evidence that mucus production by the transposed intestinal

<sup>1</sup>School of Clinical Medicine, Tsinghua University, Beijing, China

<sup>2</sup>Department of Urology, The First Hospital of Tsinghua University, Beijing, China

<sup>3</sup>Center for Stem Cell Biology and Regenerative Medicine, School of Medicine, Tsinghua University, Beijing, China

<sup>4</sup>Department of Urology, The Affiliated Hospital of Guizhou Medical University, Guiyang, Guizhou, China

\*These authors contributed equally to this work.

### Corresponding authors:

Shengwen Li, School of Clinical Medicine, Tsinghua University, No. 1, Tsinghua Yuan, Haidian District, Beijing 100084, China and Department of Urology, The First Hospital of Tsinghua University, Beijing 100016, China.  
Email: swli@mail.tsinghua.edu.cn

Jie Na, Center for Stem Cell Biology and Regenerative Medicine, School of Medicine, Tsinghua University, Beijing 100084, China.  
Email: jie.na@tsinghua.edu.cn



segments does not decrease over time in the majority of patients,<sup>4,6</sup> which may lead to a series of complications, such as recurrent urinary tract infection, stone formation, gradual renal dysfunction, pouch obstruction, urinary retention, and resultant neobladder perforation.<sup>7</sup> Several attempts have been made to address these problems. A randomized controlled trial compared the efficacy of N-acetylcysteine, aspirin, and ranitidine in reducing mucus secretion after bladder reconstruction and found there was no benefit of these drugs over the placebo.<sup>6</sup> In animal studies, attempts have been made to reduce mucus secretion by stripping off the intestinal mucosa and using seromuscular segments of the intestine.<sup>8,9</sup> However, severe fibrosis and retraction of the seromuscular segment were reported, which made this surgery not suitable for orthotopic neobladder reconstruction.

Bladder tissue engineering is considered to be the most promising alternative to solve these problems. Two major strategies of tissue engineering include the use of acellular and cellular scaffolds. Despite many encouraging reports about experimental tissue-engineered bladder reconstruction, it is still in its infancy and faces many challenges, such as the source of cells, their proliferation in vitro, the immunogenicity of synthetic grafts, biomaterials-associated mechanical properties, and fibrotic reaction.<sup>10</sup> It will take a long time to complete the translation of synthetic biomaterials into clinical settings. Autologous tissue grafts are the gold standard for comparison with other implantable biomaterials because these grafts have the properties necessary for new tissue regeneration and structural reconstruction. Additionally, the antigenicity of autologous grafts is not observed after transplantation.<sup>11</sup>

In summary, our autologous tissue-engineering approach, where the peritoneal ileal seromuscular graft was used to reconstruct the neobladder, presents a promising new strategy to reduce the complications related to urinary diversion.

## Materials and methods

### Study design and animal care

The present study was conducted in accordance with the Guide for the Care and Use of Animals for Research Purposes and was approved by the First Hospital of Tsinghua University animal ethics committee (number: RECLA18-02).

We used eight female domestic minipigs weighing between 25 and 30 kg. The pigs were divided into two groups. The experimental group received an autologous peritoneal ileal seromuscular graft-based neobladder, and the control group received a normal U-shaped ileal neobladder. Before the operation, all pigs have fasted for 12 h, and then they were given free access to water.

All operations were performed under general anesthesia and mechanical ventilation. First, ketamine (20 mg/kg) and atropine (0.05 mg/kg) were injected intramuscularly. Then

intravenous access was established through the marginal ear vein. Anesthesia was maintained with perfusion of 1 mg/kg propofol and 5 mg atracurium per hour. To prevent infection, preoperative antibiotic cefuroxime 50 mg/kg i.m. was administered. The surgical procedures were successfully performed in all eight porcine models without complications. After the operation, the pigs only received water during the first day. They were given regular food the second day. Antibiotic cefuroxime (50 mg/kg, twice a day for 7 days) was administered with food to prevent infection. The reconstructed neobladders were washed every 6 h through the urethral catheter. The ureteral stents, the silicone balloon, and the urethral catheter were removed 10 days after surgery. Only one pig in the experimental group had an infection and was euthanized 16 days after the operation. Necropsy demonstrated separation of the transplanted peritoneum from the seromuscular layer and pyonephrosis. The rest of the animals survived to the study endpoint of 3 months with no complications or adverse events.

### Surgical procedure

For the control group, the ileal neobladder was constructed as described in Koie et al.<sup>12</sup> Briefly, a 40 cm ileal segment was selected and then detubularized. The bowel loops were folded into a U configuration, and the two medial borders were then oversewn. The uretero-enteric anastomosis was performed by the Le Duc technique.

For the experimental group, to engineer an autologous graft with a suitable surface epithelium and an underlay muscle layer with sufficient elasticity and mechanical strength, we combined the peritoneal sheet from the anterior abdominal wall and the seromuscular layer from the ileum. We chose these tissues for the following reasons: (1) peritoneal tissue on the abdominal wall is abundant and closeby. (2) the ileum loop has long been used for ureteral and bladder reconstruction in clinical medicine,<sup>13</sup> the seromuscular layer of the ileum consists mostly of smooth muscle, which is easy to adapt to the desired width and provides sufficient elasticity and mechanical strength.

We prepared the peritoneal sheet from the abdominal wall as follows: a lower midline abdominal incision was made extending from the umbilicus to the pubic symphysis. The anterior rectus fascia and the transversalis fascia were incised. A 12 cm portion of peritoneum was incised in the line of the abdominal incision, and then an 8 cm portion of peritoneum was incised laterally (Figure 1(a)). Then, the peritoneal sheet was laid on top of a seromuscular layer made from the ileum.

To prepare the seromuscular layer from the ileum, a 40 cm segment of ileum, 15 cm from the ileocecal valve was chosen (Figure 1(b)). A one-centimetre incision was made in the middle of the ileum. The seromuscular layer was peeled from the submucosa on both sides of the ileum laterally, as far as the mesenteric border with forceps. Blood

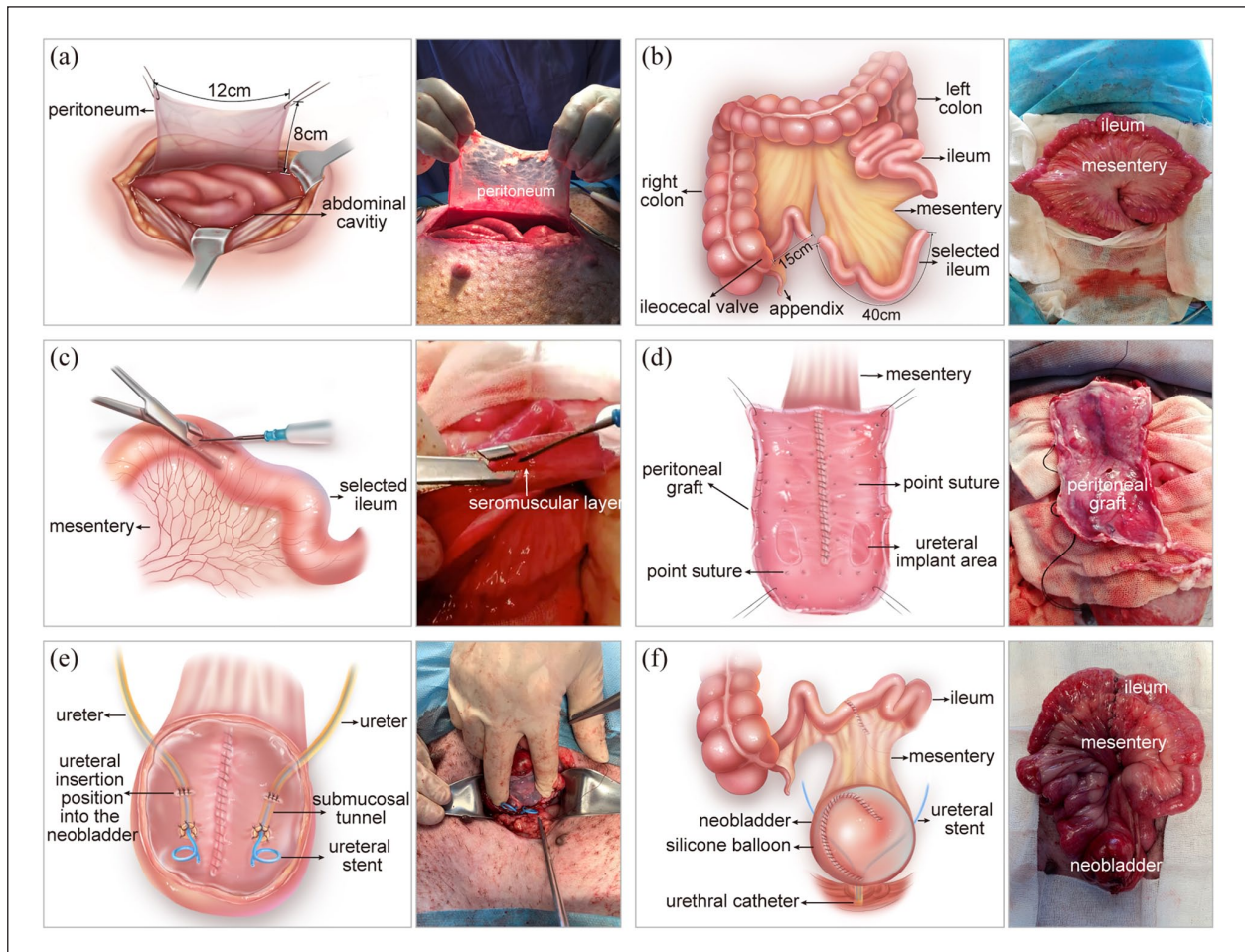


**Figure 1.** Ileal neobladder construction using the peritoneal ileal seromuscular graft: (a) preparation of the peritoneum, (b) selecting the ileal segment, (c) separating the seromuscular layer, (d) making the peritoneal ileal seromuscular graft, (e) uretero-peritoneal ileal seromuscular graft anastomosis, and (f) completing the construction of the ileal neobladder.

vessels at the mesenteric root were sealed (Figure 1(c)). The remaining ileum was joined together by anastomosis.

The seromuscular layer was folded into a U-shaped suture, and the opposite inner borders were sewn together with 3–0 absorbable sutures to assemble the peritoneal-seromuscular graft. After the anastomosis was completed, the area of the seromuscular layer was approximately  $8 \times 12 \text{ cm}^2$ . The peritoneum piece was transferred onto the seromuscular layer. The peritoneum edge was approximated to the edge of the seromuscular layer with a 5–0 absorbable suture, ensuring that both tissues were incorporated with each other (Figure 1(d)).

Afterwards, we removed the entire bladder and replaced it with the neobladder made from the peritoneal graft. The peritoneal graft prepared above was sutured with the ureter using the submucosal tunnelling technique and then sutured with the urethra, which is commonly practised in bladder reconstruction surgeries (Figure 1(e)). A 4.7Fr ureteral catheter was placed in each ureter and fixed through the wall of the neobladder. We placed a silicone

balloon containing 100 mL sterile saline solution in the neobladder. The silicone balloon can support the neobladder and pressure the peritoneal graft to prevent the detachment of the mesothelial sheet from the seromuscular layer. We also placed a 14Fr urethral catheter in the urethra. The ureteral stents and the silicone balloon were tied to the urethral catheter (Figure 1(f)). So, they could be taken out together 10 days after the surgery.

### *Imaging, physiology, blood and urine tests*

All animals received intravenous urogram (IVU), cystograms, and cystometrograms under light general anaesthesia 3 months after surgery. The bladder capacity and function of the neobladder were examined. Blood biochemistry, including creatinine, blood urea nitrogen (BUN), chloride, sodium, and potassium levels, were analysed before surgery and at the sacrifice. Venous gas analysis and urine samples were also obtained at the same time points and analysed.

### Histology and immunohistochemistry

After physiology test, blood and urine sample collection, pigs were euthanized, and their neobladders were harvested for histological analysis. The harvested neobladder tissues were fixed in 10% formalin for 1 week, then embedded with paraffin and sliced into 5  $\mu$ m sections. Haematoxylin and eosin (H&E) stains were performed according to standard procedures. Immunohistochemical (IHC) analysis was performed using the mouse monoclonal antibody against cytokeratin 7 (CK7) (1:100, ab9021, Abcam), Uroplakin III (UPK3) (1:20, ab78196, Abcam) and alpha smooth muscle actin ( $\alpha$ -SMA) (1:200, A5228, Sigma-Aldrich). The staining was performed according to the manufacturer of the mouse and rabbit specific HRP/DAB detection IHC kit (ab64264, Abcam). Images were obtained using the Panoramic Scanner system (3D HISTECH, Ltd., Budapest, Hungary).

### Transcriptomic analysis

Three months after surgery, normal peritoneum (NP), the mucosa of the normal bladder (MNB), the mucosa of neobladder from the experimental group (MN-Exp), and mucosa of neobladder from the control group (MN-Ctrl) were collected separately. Total RNA was extracted from the fresh tissues with the RNeasy Plus Mini Kit (Qiagen) according to the manufacturer's instructions and treated with RNase-free DNase. RNA-seq libraries were prepared using Smart-seq2<sup>14</sup> as the manufacturer's instructions, and the cDNAs were subject to library preparation with TruePrep DNA Library Prep Kit V2 for Illumina (Vazyme, TD502-01). The sequencing was performed by HiSeq X Ten (Illumina). Reads were trimmed with the trim\_galore software with the default parameter. Then, the reads were mapped to Sscrofa11.1 whole genome using hisat2 with parameter -p 16. We counted for each gene how many reads mapped to it using htseq-count version 0.11.1 with parameters -r pos -a 10 -t exon -s no -i gene\_id -m union. And the differentially expressed genes were identified by DESeq2 software with several criteria ( $|\log_2fc| \geq 1$  and false discovery rate [FDR]  $\leq 0.05$ ). GO term enrichment was analyzed using ClusterProfiler.<sup>15</sup> RNA-seq data was submitted to the National Center for Biotechnology Information under accession number GSE145751.

### Statistical analysis

The data were presented as the mean  $\pm$  standard deviation (M  $\pm$  SD). Statistical analysis was performed using GraphPad Prism 7.0 software (GraphPad Software, San Diego, CA, USA). Unpaired two-tailed *t*-test was used to compare two groups. *p*-value (*p*) < 0.05 was considered statistically significant.

## Results

### Neobladders made from peritoneal-graft have similar bladder function to that of the ileum-based neobladder

All the animals survived the surgery. The control group and the experimental group have similar body weight before and after the surgery (Figure 2(a)). The operation time was about 1 h longer for the experimental group than the control group ( $325 \pm 13.2$  min vs  $248 \pm 13.8$  min, *p* = 0.007) (Figure 2(b)), as the new method required extra time to construct the peritoneal-ileal seromuscular graft. Ten days after the surgery, the catheters and the silicone balloon were removed together. Then the animals began to urinate normally. We measured renal function (Figure 2(c) and (d)), serum electrolytes (Figure 2(g)–(i)), and the urine white blood cells (Figure 2(m)) before and 3 months post-operation and found there was no significant difference. However, the serum pH levels became slightly more acidic, mean = 7.32 in the control group versus 7.39 in the experimental group (*p* = 0.016), 3 months after the surgery (Figure 2(e)). This result implied that animals in the control group had a higher risk of acidosis. In addition, urine samples collected 1 week and 3 months after the surgery showed that the transposed intestinal segments secreted mucus continuously in the control group (Supplemental Figure 1). Three months after surgery, the mean capacity of neobladders in the experimental group ( $529.8 \pm 34.5$  mL) was slightly lower than that of the control group ( $580.3 \pm 17.7$  mL), but no statistical significance (*p* = 0.241) (Figure 2(j)). No statistically significant differences in pressure (Figure 2(k)) and compliance (Figure 2(l)) were found between groups.

Postoperative intravenous urogram (IVU) revealed that the urinary tracts were patent, and there was no hydronephrosis and dilated ureter in pigs (Figure 3(a) and (d)). Cystograms revealed that all the neobladders had a spherical shape, and there was no evidence of contrast extravasation (Figure 3(b) and (e)). The above results strongly suggested that all the neobladder functioned normally.

### Gross examination revealed better morphological characteristics of neobladder in the experimental group

Three months after the surgery, a visual examination found that the neobladder wall in all survived pigs healed completely (Figure 4). No stricture was noted at the uretero-enteric anastomosis. In the control group, the luminal surface of the neobladder was similar to that of normal ileum with many folds, and one pig developed a large stone (1.0 cm  $\times$  1.0 cm) in the neobladder made from the ileum alone (Figure 4(a)). Surprisingly, the neobladder made from the peritoneal graft (the experimental group) showed a smooth luminal surface, no stones were found (Figure 4(b)), and it appeared similar to that of the normal bladder

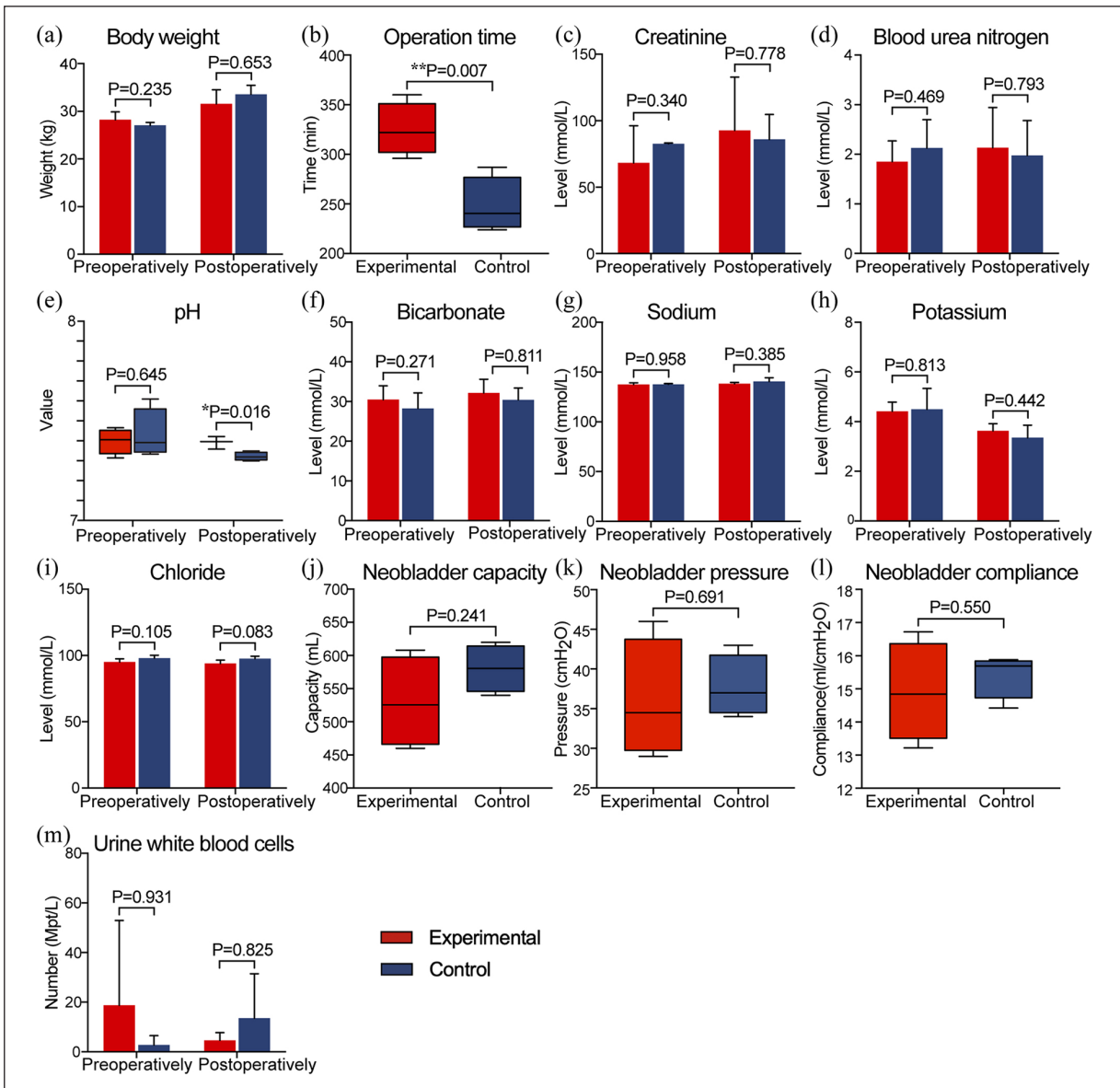


**Figure 2.** The summary of perioperative results. Differences in body weight (a) between the two groups were not statistically significant, (b) The average operation time was significantly higher in the experimental group. Blood biochemical examination showed normal renal function (c and d) and electrolytes (g–i) in both groups. (e and f) Venous gas analysis revealed the pH level in controls was significantly lower than that in the experimental group. There were no statistically significant differences in neobladder capacity (j), pressure (k), and compliance (l) between the two groups. Urine analysis (m) showed no signs of urinary tract infection in both groups. (\* $p < 0.05$ , \*\* $p < 0.01$ ).

(Figure 4(c)), suggesting that the mesothelium in the graft has formed a proper barrier on top of the seromuscular layer from the ileum. There were no signs of visible leakage and infection in any of the survived pigs' peritoneal cavity.

#### *The mesothelium on the peritoneal graft transformed into urothelium-like cells in the neobladder*

Figure 5A and B show the staining of the peritoneal sheet and the intact ileal seromuscular layer, respectively. We

performed histological analysis of the neobladder from the control and the experimental group. Strikingly, HE staining of the sections from the peritoneal graft neobladder was very similar to the normal bladder tissues (Figure 5C(a)). A thick layer of urothelium-like cells lined on the neobladder's luminal surface (Figure 5C(d)) in the experimental group. Immunohistochemistry (IHC) staining revealed that urothelium-like cells in the experimental group expressed urothelial cell-typical marker proteins, UPK3 and CK7 (Figure 5C(b), (c), (e) and (f)). In contrast, no positive staining was detected in the control group's epithelial layer

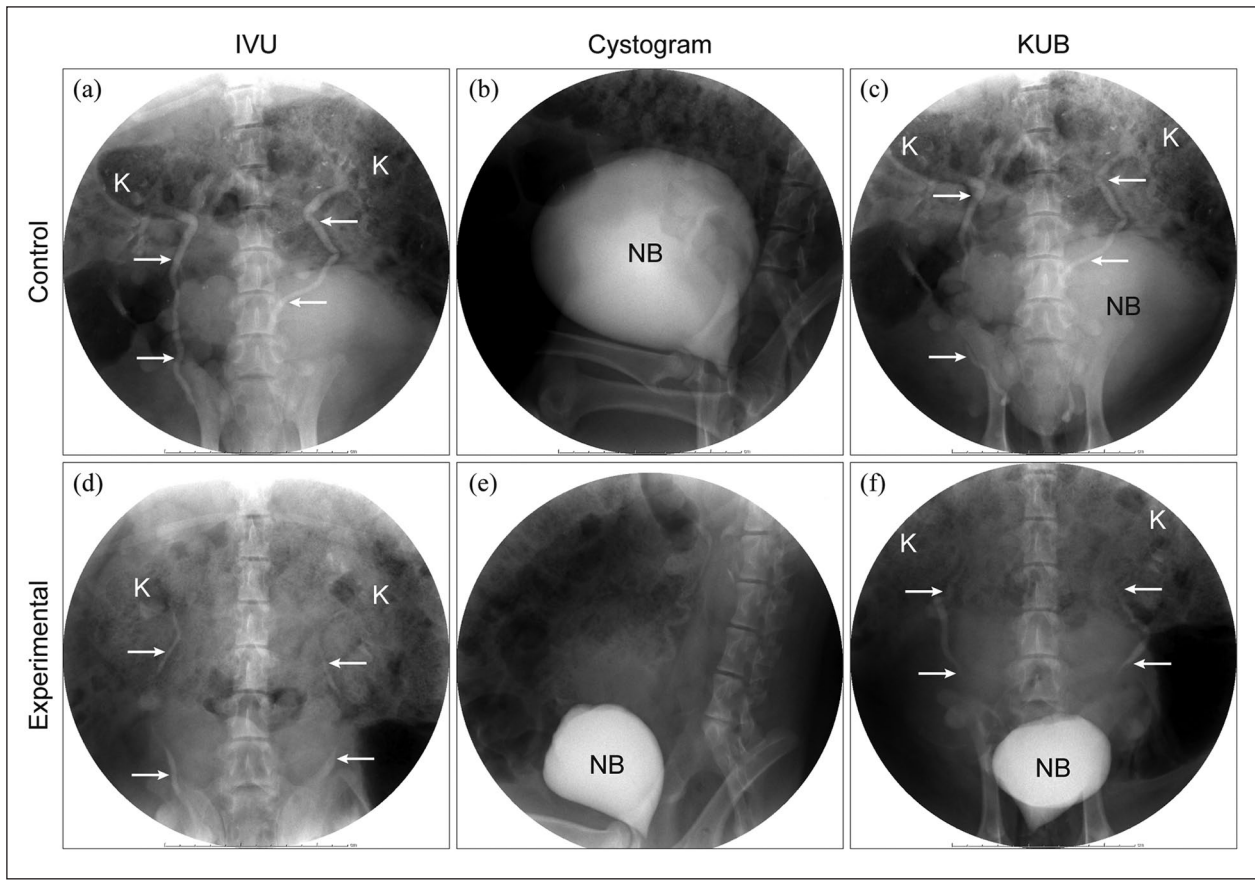


**Figure 3.** Postoperative intravenous urography (IVU) 5 min following the instillation of 50 mL of intravenous iohexol, which demonstrated no obstruction in both groups (a and d). Postoperative cystograms showed the spherical neobladder and no evidence of contrast extravasation was noted in both groups (b and e). Kidney, ureter and neobladder were included simultaneously in the KUB image (c and f).

K: kidney; white arrow: ureter; NB: neobladder.

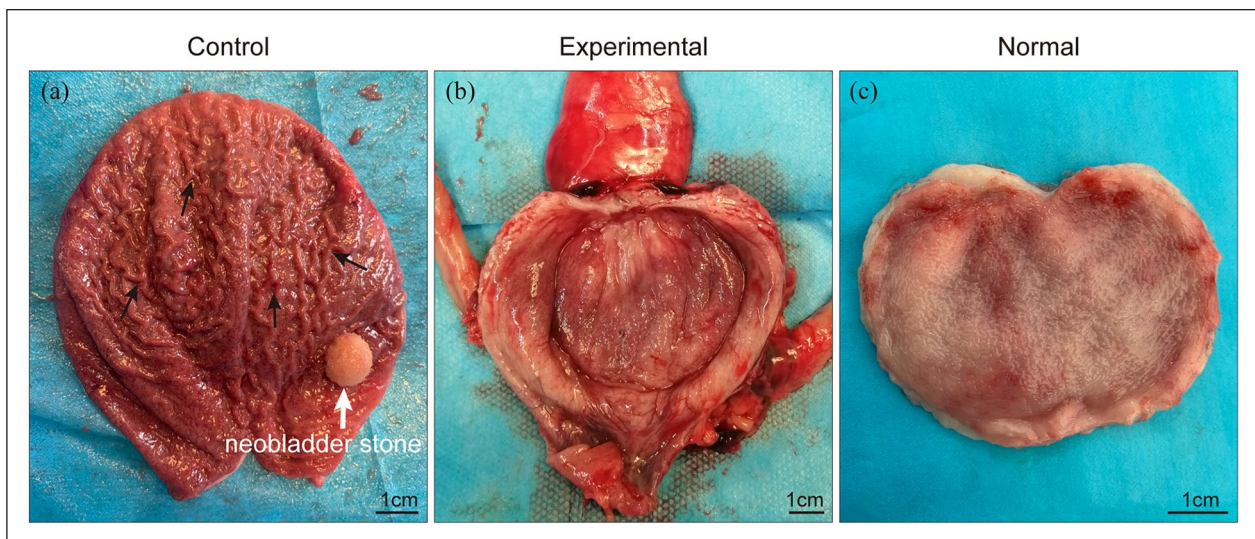


**Figure 4.** Gross examination revealed complete healing of the neobladder wall in surviving pigs: (a) the luminal surface of the neobladder was similar to that of normal ileum with many folds (black arrow) and one pig developed neobladder stone (white arrow) and (b) the luminal surface of the neobladder was smooth, no stones were found, and it was similar to that of the normal bladder (c).

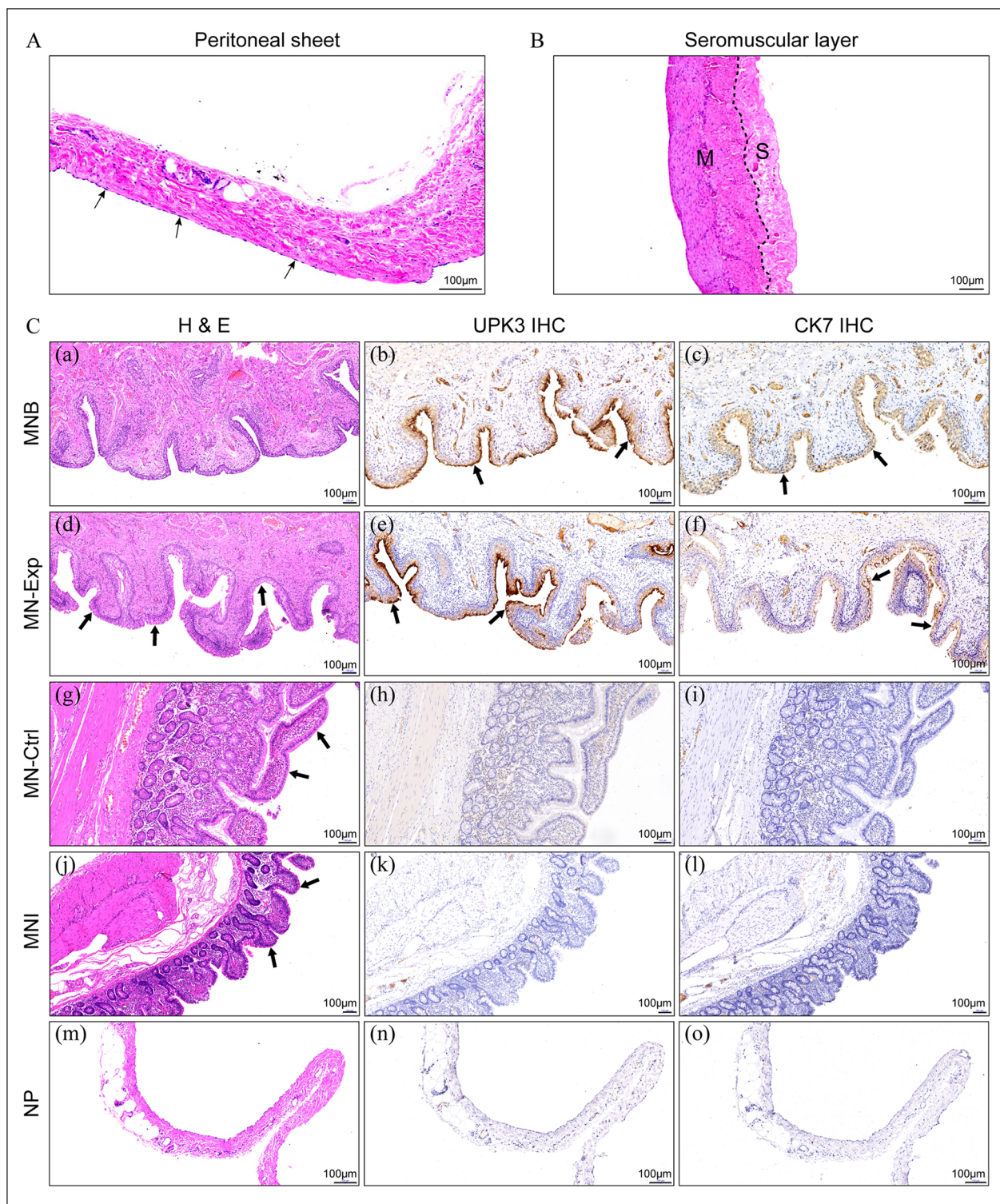


**Figure 5.** A. HE staining of the peritoneal sheet. Black arrow: mesothelial cells. B. HE staining of the intact ileal seromuscular layer. M: muscle layer; S: serosa layer. C. Histopathological assessment of the neobladder constructed by both methods. Similar to what was observed in the MNB (a), HE staining revealed a thick layer of urothelium-like cells lying on the luminal surface of MN-Exp (d) (black arrow). Immunohistochemical analysis showed UPK3 and CK7 were highly expressed in the MNB (b and c) and MN-Exp (e and f) (black arrow), while no such changes were observed in the MN-Ctrl (h and i) and MNI (k and l). Compared with the MNI (j), the villi marked by the black arrow in the MN-Ctrl (g) were not atrophied 3 months after surgery. UPK3 (n) and CK7 (o) were negative on the NP (m). MNB, mucosa of the normal bladder; MNExp, mucosa of the neobladder in the experimental group; MN-Ctrl, mucosa of the neobladder in controls; MNI, mucosa of the normal ileum; NP, normal peritoneum; UPK3, uroplakin III; CK7, cytokeratin 7.

(Figure 5C(h), (i), (k) and (l)). Moreover, HE staining revealed that even after 3 months, the ileum villi in the control neobladder (Figure 5C(g)) have not atrophied and was similar to the villi on the mucosa of normal ileum (Figure 5C(j)). An enlarged view of the HE stained neobladder of the two groups is shown in Supplemental Figure 2. IHC showed that muscle cells in both groups were positive for  $\alpha$ -SMA (Supplemental Figure 3). The muscle distribution of the neobladder in the experimental group was similar to that of the normal bladder.

### *Transcriptomic analyses revealed a similarity between the mucosa of the peritoneal graft and the mucosa of the normal bladder*

To find out whether the peritoneal graft has indeed developed urothelium-like cells, we performed transcriptome profiling of the mucosa of the neobladder in the experimental group (MN-Exp), the mucosa of the neobladder in the control group (MN-Ctrl), the mucosa of the normal bladder (MNB) and normal peritoneum (NP). Scatter plots comparing gene expression levels between MN-Exp, MN-Ctrl, MNB, and NP cells revealed that MN-Exp and MNB cells were the most similar pair with the highest coefficient of determination ( $R^2$ ). They were highly divergent from MN-Ctrl or NP cells (Figure 6(a)). In line with these results, hierarchical cluster analysis also showed a high degree of similarity between MN-Exp and MNB cells but significant differences between them and the NP or MN-Ctrl group (Figure 6(b)). We also performed additional clustering analysis comparing the transcriptome of MN-Ctrl, NP, MN-Exp, and MNB (Supplemental Figure 4). Consistent with the hierarchical cluster analysis, mucosa cells from MN-Exp and MNB were the most closely clustered, then with mucosa cells from NP, but not similar to cells from the MN-Ctrl, essentially the ileum epithelium (Supplemental Figure 4). The gene list of each cluster was provided in Supplemental Table 1. We selected cluster 2 genes highly expressed in both MN-Exp and MNB, and did GO analysis. Cluster 2 contained many genes associated with epithelial development and bladder function, such as morphogenesis of a branching epithelium, cell-cell junction organization, regulation of NF-kappa B signaling, urogenital system development and regulation of nucleobase-containing compound metabolic process (Figure 6(c)). A full list of cluster 2 GO terms is provided in Supplemental Table 2. These results indicate that MN-Exp cells had a molecular signature of bladder epithelium-like cells and adopted corresponding metabolism and proliferation characteristics. We next checked the expression levels of marker genes of the bladder mucosa, UPK1a, UPK1b, UPK2, UPK3a,<sup>16–18</sup> and KRT family genes, which highly expressed in normal MNB to form the epithelial cytoskeleton.<sup>19</sup> The result showed that the expression levels of these marker genes in the MN-Exp

group were comparable to those of MNB, but not the other two groups (Figure 6(d)). We also analyzed the gene expression differences between MN-Exp and NP, and the result showed that they expressed many different genes (Figure 6(e)). Gene Set Enrichment Analysis (GSEA) revealed that genes significantly upregulated in the MN-Exp were enriched for keratinization/epithelial cell differentiation terms ( $FDR < 0.05$ ), water homeostasis, and nucleobase containing compounds transporter activity (Figure 6(f)), which is in agreement with the property and function of urothelium cells, but not peritoneum cells. Sum above, our transcriptomic analysis strongly suggests that the peritoneal graft has developed urothelium-like cells.

## **Discussion**

In this study, we describe a novel autologous tissue engineering strategy to avoid the complications caused by transposed intestinal segments. Surprisingly, the neobladder's epithelial layer made from the peritoneal graft appeared highly similar to that of a normal bladder. The histopathological analysis demonstrated that the peritoneal graft contained an epithelial layer highly similar to the urothelium. We also compared the transcriptome of the mucosa layer from the peritoneal graft neobladder to that from several control groups. The results are consistent with the morphology change. To our knowledge, this is the first transcriptome study to analyze the change in tissue identity after autologous tissue transplantation in the bladder.

Free peritoneal grafts or patches used for urological tissue reconstruction have been documented in several studies. Shaul et al.<sup>20</sup> reported their successful experience with tubularized peritoneal free grafts for urethroplasty in rabbits. Histological analysis demonstrated that a multi-layered epithelium similar to the urothelium replaced the peritoneal mesothelium 2 weeks after grafting. Yifeng et al.<sup>21</sup> created ureteral mucosa substitutes using free tubularized peritoneal grafts in a dog model. After 10 weeks, histological examination showed that the constructed ureteral lumens were lined with transitional epithelium. Brandao et al.<sup>22</sup> performed robotic ureteral reconstruction with a tubularized peritoneal flap in six pigs and reported focal urothelial lining of the neoureter. In our study, we removed the entire bladder and replaced it with a neobladder assembled from the peritoneal sheet and the seromuscular layer of the ileum. Three months later, we observed urothelium-like cells on the luminal surface of the neobladder in the experimental group, and the RNA-seq data showed the mucosa from the experimental group (MN-Exp) has a similar transcriptomic signature with the mucosa of the normal bladder (MNB) (Figure 6). However, the exact mechanism of this phenomenon remains unknown.

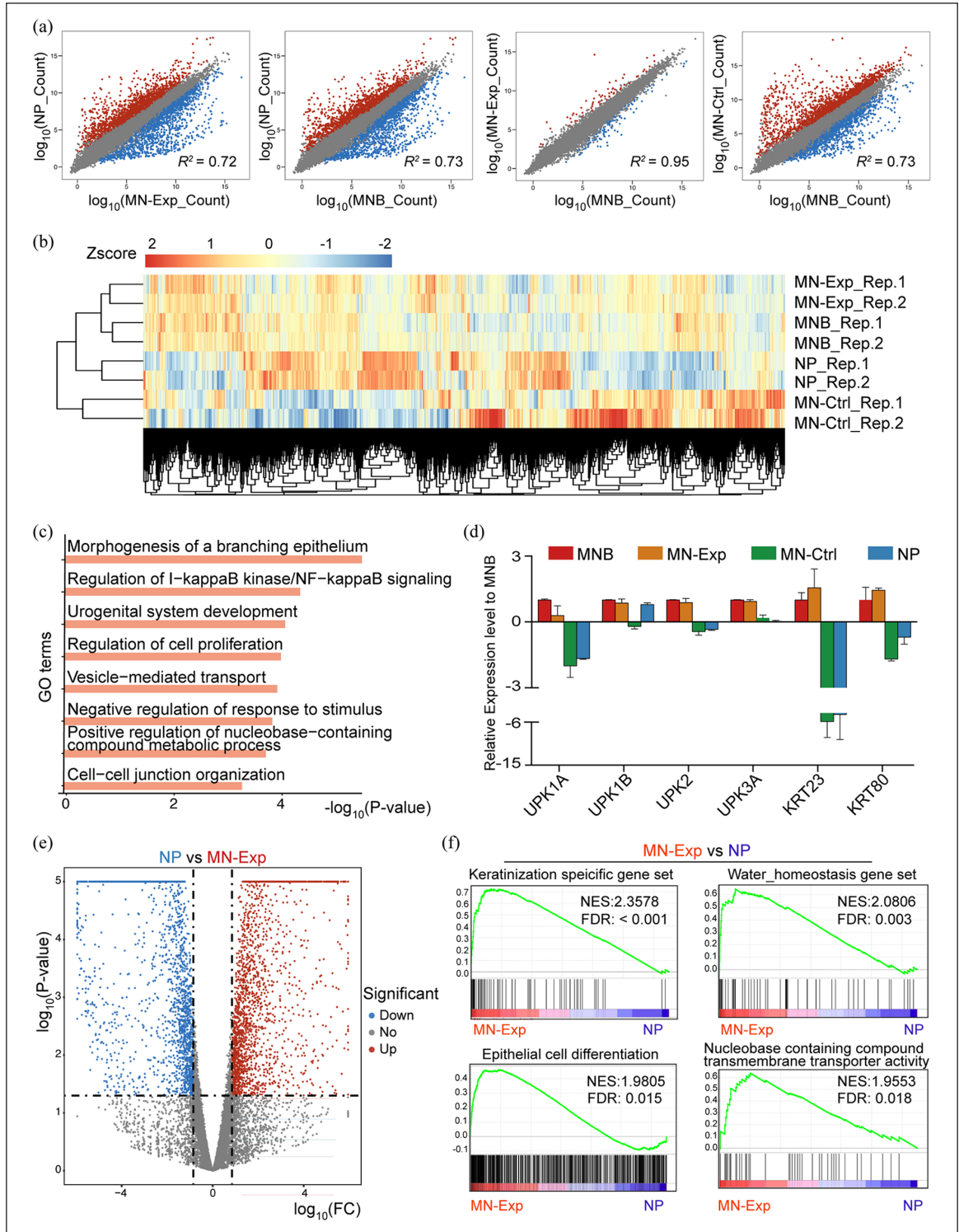


**Figure 6.** Global gene expression profiles of MN-Exp, MNB, NP, MN-Ctrl: (a) pairwise scatter plot analysis of the global gene expression profiles of MN-Exp, MNB, NP, MN-Ctrl cells. The transcriptome of each cell type was profiled by RNA-seq analysis. Gene reads count levels are depicted in  $\log_{10}$  scale. Pearson's correlation coefficients ( $r$ ) are indicated, (b) heat map of the z-transformed gene expression values in MN-Exp, MNB, NP, MN-Ctrl. MN-Exp, MNB cells are classified into the same hierarchical cluster, (c) GO enrichment of genes highly expressed in both MNB and MN-Exp compared to MN-Ctrl and NP, (d) expression of MNB cell marker genes UPK family and KRT family genes. Data are presented as mean  $\pm$  SD ( $n=2$ ), (e) volcano plot (significance vs. fold change) of significantly altered genes (fold change  $\geq 2$  and  $p$ -value  $< 0.05$ ) between NP and MN-Exp cells, and (f) Gene Set Enrichment Analysis (GSEA) showed significant enrichment of epithelial related gene sets, water homeostasis and nucleobase containing compounds transporter activity in MN-Exp compared to NP. The normalized enrichment scores (NES) and tests of statistical significance (FDR) are shown.

The peritoneum is a semi-permeable membrane covering the abdominal wall and most abdominal organs. It comprises a single layer of mesothelial cells (MCs) and the underlying submesothelial connective tissue.<sup>23</sup> Mesothelial cells have been shown to induce tissue repair.<sup>24</sup> Some studies have reported that MCs can differentiate into myofibroblasts, smooth muscle cells, adipocytes, and osteoblasts under specific *in vitro* conditions.<sup>25</sup> For example, Liu et al.<sup>26</sup> found that, after treatment with fibroblast-associated growth factor or exposure to injury, MCs have undergone epithelial-mesenchymal transition. Accumulating evidence supports the concept that adult MCs retain the ability of embryonic mesoderm multi-lineage differentiation and can represent the population of primitive mesoderm stem cells.<sup>27</sup> This plasticity of MCs has generated considerable interest among investigators in the field of cell therapy and tissue engineering. The submesothelial connective tissue mainly contains fibroblasts, adipocytes, blood, and lymphatic vessels. Several studies have discovered progenitor cells similar to mesenchymal stem cells in the submesothelium.<sup>25,28</sup> These progenitor cells have also been used for bone tissue engineering.<sup>28</sup> Furthermore, an epigenetic study established that dramatic changes in the environment may initiate *in vivo* reprogramming of differentiated cells.<sup>29</sup> Based on the evidence above, we propose two possible hypotheses. First, peritoneal mesothelial cells may transdifferentiate into urothelium-like cells in the urine environment. Second, peritoneal progenitor cells may directionally differentiate into urothelium-like cells by paracrine signals. This complex mechanism needs to be further confirmed *in vitro* experiments using 3D cell culture models.

The urothelium is a stratified epithelium that changes in appearance according to the degree of distension of the bladder. The cells in the urothelium are composed of at least three layers.<sup>30</sup> The stratified urothelium provides a strong permeability barrier throughout the urinary tract. This barrier function limits the transfer of ions and solutes across the urothelium and protects the subjacent tissue against damage from toxic urine components.<sup>31</sup> Expression and assembly of crystalline protein uroplakins into heterodimers, which form hexagonal plaques at the apical cell surface, is critical for maintaining the integrity and function of the urothelial permeability barrier.<sup>32</sup> Our histopathological analysis revealed that MN-Exp could transform into urothelial like tissues. Besides, transcriptomic analyses indicated that MN-Exp highly expressed the uroplakin family genes, and the expression level was similar to that of MNB, confirming that the differentiated cells on the MN-Exp had the ability to form plaques and then involved in maintaining the barrier function.

Several different types of stem cells, including urine-derived stem cells (USCs),<sup>31</sup> adipose tissue-derived stem cells (ADSCs),<sup>33</sup> bone marrow mesenchymal stem cells (BMSCs),<sup>34</sup> embryonic stem cells (ESCs) and induced

pluripotent stem cells (iPSCs),<sup>18</sup> have been investigated for urothelial cell differentiation. The physiological process of urothelial cell differentiation is complex and may involve signaling pathways, various structural elements, the cellular environment, and trophic factors.<sup>35</sup> For example, peroxisome proliferator-activated receptor- $\gamma$  (PPARG) could modulate mitochondrial gene expression and promote bladder epithelial cell differentiation.<sup>36</sup> Retinoic acid, a potent signaling molecule, could regulate specification and regeneration of the urothelium in progenitors.<sup>37</sup> In addition, hedgehog/Wnt signaling, acting across the epithelial-stromal boundary, supports regenerative proliferation of bladder epithelial cells.<sup>38</sup> There is also evidence that microRNA miR-205 may contribute to regulating urothelial differentiation by modulating the expression of tight junction-related proteins.<sup>39</sup> Growth factors, such as vascular endothelial growth factor (VEGF) and epidermal growth factor (EGF), have also been reported to promote urothelial differentiation.<sup>40,41</sup>

Keratins are generally regarded as epithelial cell markers. However, it has recently been shown that Krt23, one of the peroxisome proliferator-activated receptor- $\alpha$  (PPARA) target genes, also play a significant role in inducing cellular signalling pathways.<sup>42</sup> One study demonstrated that Krt80 was closely linked to the differentiation process and helped to maintain the stability of the plasma membrane of differentiated cells.<sup>43</sup> In our study, Krt23 and Krt80 were highly expressed in the experimental group, which indicated both of these proteins might be involved in the urothelial differentiation.

To our knowledge, this investigation is the first to use autologous peritoneal grafts to reengineer and regenerate the bladder. Despite the promising outcome, this study leaves several things to be desired. For example, only a relatively small number of animals were used. Despite that, we believe using large animal models, such as pigs, for tissue engineering research is of special importance. Additionally, the neobladder's innervation remains a challenging problem today. It is difficult to explain why pigs can urinate spontaneously after the catheter is removed. We think the pigs are likely able to control urination by adjusting the abdominal pressure. Better animal models are needed for urodynamic assessment because anesthesia can impair the lower urinary tract function and affect the outcome.<sup>44</sup> Furthermore, this procedure requires approximately one more hour to create the peritoneal ileal seromuscular graft. Nevertheless, we believe that mucus-free urine and the reduction in metabolic complications are substantial long-term benefits that outweigh the extra operating time.

## Conclusion

In summary, the use of tissue-engineered peritoneal grafts for bladder reconstruction is shown to be technically

feasible and reproducible in a porcine model. Autologous peritoneum can serve as a source of autologous cells or materials for tissue engineering of the internal organs. Further studies are required to assess this novel procedure's long-term functional outcomes and explore the exact mechanism of urothelium-like cells appeared in the neobladder.

### Acknowledgements

The authors would like to thank Chao Wang, Fei Han, Hao Wu, Shuaijun Wang, Xinzi Wu, Yonglin Zhu, Hui Qiu, and Rujin Huang for their technical contributions to the experiments in this study. Many thanks to Jiaxin Zhao for drawing the surgical illustrations.

### Author contributions

BC, XC, JS, JN, and SL conceived the study and designed the experiments. BC, WW, ZS, HJ, FZ, JW, and SL performed surgery and tissue transplantation studies; XC performed RNA-seq library construction and bioinformatics analysis; BC, XC, JN, and SL wrote the manuscript. All authors read and approved the final version of the manuscript.

### Declaration of conflicting interests

The author(s) declared no potential conflicts of interest with respect to the research, authorship, and/or publication of this article.

### Funding

The author(s) disclosed receipt of the following financial support for the research, authorship, and/or publication of this article: This study was supported by the National Key R&D Program of China Grant 2017YFA0102802 and 2019YFA0110001 to JN, and Chow Tai Fook Medical Research Special Fund (grant number: 202836019-04).

### Ethical approval

This article does not contain any studies with human subjects performed by any of the authors. All animal experiments were conducted in accordance with the Guide for the Care and Use of Animals for Research Purposes and approved by the First Hospital of Tsinghua University animal ethics committee (number: RECLA18-02).

### ORCID iD

Jie Na  <https://orcid.org/0000-0003-1820-0548>

### Data availability

Raw and processed RNA-seq data are publicly available at the Gene Expression Omnibus (GEO) with accession number GSE145751. All other relevant data are available from the corresponding author upon request.

### Supplemental material

Supplemental material for this article is available online.

### References

1. Bray F, Ferlay J, Soerjomataram I, et al. Global cancer statistics 2018: GLOBOCAN estimates of incidence and mortality worldwide for 36 cancers in 185 countries. *CA Cancer J Clin* 2018; 68: 394–424.
2. Lerner SP. Bladder cancer: ASCO endorses EAU muscle-invasive bladder cancer guidelines. *Nat Rev Urol* 2016; 13: 440–441.
3. Hautmann RE, Abol-Enein H, Lee CT, et al. Urinary diversion: how experts divert. *Urology* 2015; 85: 233–238.
4. Murray K, Nurse DE and Mundy AR. Secreto-motor function of intestinal segments used in lower urinary tract reconstruction. *Br J Urol* 1987; 60: 532–535.
5. Hautmann RE, de Petriconi RC and Volkmer BG. 25 years of experience with 1,000 neobladders: long-term complications. *J Urol* 2011; 185: 2207–2212.
6. N'dow J, Robson CN, Matthews JN, et al. Reducing mucus production after urinary reconstruction: a prospective randomized trial. *J Urol* 2001; 165: 1433–1440.
7. Amini E and Djaladat H. Long-term complications of urinary diversion. *Curr Opin Urol* 2015; 25: 570–577.
8. Salle JLP, Fraga JCS, Lucib A, et al. Seromuscular enterocystoplasty in dogs. *J Urol* 1990; 144: 454–456.
9. De Badiola F, Ruiz E, Puigdevall J, et al. Sigmoid cystoplasty with argon beam without mucosa. *J Urol* 2001; 165: 2253–2255.
10. Adamowicz J, Pokrywczynska M, Van Breda SV, et al. Concise review: tissue engineering of urinary bladder; we still have a long way to go? *Stem Cells Transl Med* 2017; 6: 2033–2043.
11. Chen FM and Liu X. Advancing biomaterials of human origin for tissue engineering. *Prog Polym Sci* 2016; 53: 86–168.
12. Koie T, Hatakeyama S, Yoneyama T, et al. Experience and functional outcome of modified ileal neobladder in 95 patients. *Int J Urol* 2006; 13: 1175–1179.
13. Torbey K and Leadbetter WF. The use of the seromuscular layer of an ileal loop for ureteral replacement. *J Urol* 1962; 88: 746–757.
14. Picelli S, Faridani OR, Bjorklund AK, et al. Full-length RNA-seq from single cells using Smart-seq2. *Nat Protoc* 2014; 9: 171–181.
15. Yu G, Wang L-G, Han Y, et al. clusterProfiler: an R package for comparing biological themes among gene clusters. *OMICS* 2012; 16: 284–287.
16. Carpenter AR, Becknell MB, Ching CB, et al. Uroplakin 1b is critical in urinary tract development and urothelial differentiation and homeostasis. *Kidney Int* 2016; 89: 612–624.
17. Habuka M, Fagerberg L, Hallstrom BM, et al. The urinary bladder transcriptome and proteome defined by transcriptomics and antibody-based profiling. *PLoS One* 2015; 10: e0145301.
18. Osborn SL, Thangappan R, Luria A, et al. Induction of human embryonic and induced pluripotent stem cells into urothelium. *Stem Cells Transl Med* 2014; 3: 610–619.
19. Southgate J, Hutton KA, Thomas DF, et al. Normal human urothelial cells in vitro: proliferation and induction of stratification. *Lab Invest* 1994; 71: 583–594.

20. Shaul DB, Xie HW, Diaz JF, et al. Use of tubularized peritoneal free grafts as urethral substitutes in the rabbit. *J Pediatr Surg* 1996; 31: 225–228.
21. Yifeng J, Shujie X, Hongbin S, et al. Use of free peritoneal and bladder mucosal grafts as ureteral mucosa substitutes for management of avulsion of the ureteral mucosa in a dog model. *J Endourol* 2008; 22: 729–734.
22. Brandao LF, Laydner H, Akca O, et al. Robot-assisted ureteral reconstruction using a tubularized peritoneal flap: a novel technique in a chronic porcine model. *World J Urol* 2017; 35: 89–96.
23. do Amaral RJ, Benac P, Andrade LR, et al. Peritoneal submesothelial stromal cells support hematopoiesis and differentiate into osteogenic and adipogenic cell lineages. *Cells Tissues Organs* 2015; 200: 118–131.
24. Isaza-Restrepo A, Martin-Saavedra JS, Velez-Leal JL, et al. The peritoneum: beyond the tissue – a review. *Front Physiol* 2018; 9: 738.
25. do Amaral R, Arcanjo KD, El-Cheikh MC, et al. The peritoneum: health, disease, and perspectives regarding tissue engineering and cell therapies. *Cells Tissues Organs* 2017; 204: 211–217.
26. Liu Y, Dong Z, Liu H, et al. Transition of mesothelial cell to fibroblast in peritoneal dialysis: EMT, stem cell or bystander? *Perit Dial Int* 2015; 35: 14–25.
27. Lachaud CC, Rodriguez-Campins B, Hmadcha A, et al. Use of mesothelial cells and biological matrices for tissue engineering of simple epithelium surrogates. *Front Bioeng Biotechnol* 2015; 3: 117.
28. Shen J, Nair A, Saxena R, et al. Tissue engineering bone using autologous progenitor cells in the peritoneum. *PLoS One* 2014; 9: e93514.
29. Lay FD, Triche TJ Jr, Tsai YC, et al. Reprogramming of the human intestinal epigenome by surgical tissue transposition. *Genome Res* 2014; 24: 545–553.
30. de Graaf P, van der Linde EM, Rosier P, et al. Systematic review to compare urothelium differentiation with urethral epithelium differentiation in fetal development, as a basis for tissue engineering of the male urethra. *Tissue Eng Part B Rev* 2017; 23: 257–267.
31. Wan Q, Xiong G, Liu G, et al. Urothelium with barrier function differentiated from human urine-derived stem cells for potential use in urinary tract reconstruction. *Stem Cell Res Ther* 2018; 9: 304.
32. Tu DD, Chung YG, Gil ES, et al. Bladder tissue regeneration using acellular bi-layer silk scaffolds in a large animal model of augmentation cystoplasty. *Biomaterials* 2013; 34: 8681–8689.
33. Ling Q, Wang T, Yu X, et al. UC-VEGF-SMC Three Dimensional (3D) nano scaffolds exhibits good repair function in bladder damage. *J Biomed Nanotechnol* 2017; 13: 313–323.
34. Ning J, Li C, Li H, et al. Bone marrow mesenchymal stem cells differentiate into urothelial cells and the implications for reconstructing urinary bladder mucosa. *Cytotechnology* 2011; 63: 531–539.
35. Birder L and Andersson KE. Urothelial signaling. *Physiol Rev* 2013; 93: 653–680.
36. Liu C, Tate T, Batourina E, et al. Pparg promotes differentiation and regulates mitochondrial gene expression in bladder epithelial cells. *Nat Commun* 2019; 10: 4589.
37. Gandhi D, Molotkov A, Batourina E, et al. Retinoid signaling in progenitors controls specification and regeneration of the urothelium. *Dev Cell* 2013; 26: 469–482.
38. Shin K, Lee J, Guo N, et al. Hedgehog/Wnt feedback supports regenerative proliferation of epithelial stem cells in bladder. *Nature* 2011; 472: 110–114.
39. Chung PJ, Chi LM, Chen CL, et al. MicroRNA-205 targets tight junction-related proteins during urothelial cellular differentiation. *Mol Cell Proteomics* 2014; 13: 2321–2336.
40. Burgu B, McCarthy LS, Shah V, et al. Vascular endothelial growth factor stimulates embryonic urinary bladder development in organ culture. *BJU Int* 2006; 98: 217–225.
41. Bharadwaj S, Liu G, Shi Y, et al. Multipotential differentiation of human urine-derived stem cells: potential for therapeutic applications in urology. *Stem Cells* 2013; 31: 1840–1856.
42. Kim D, Brocker CN, Takahashi S, et al. Keratin 23 is a peroxisome proliferator-activated receptor alpha-dependent, MYC-amplified oncogene that promotes hepatocyte proliferation. *Hepatology* 2019; 70: 154–167.
43. Langbein L, Eckhart L, Rogers MA, et al. Against the rules: human keratin K80. *J Biol Chem* 2010; 285: 36909–36921.
44. Sartori AM, Kessler TM and Schwab ME. Methods for assessing lower urinary tract function in animal models. *Eur Urol Focus*. Epub ahead of print January 2020 DOI: 10.1016/j.euf.2019.12.004.